Adv. Radio Sci., 15, 61–67, 2017
https://doi.org/10.5194/ars-15-61-2017

Advances in Radio Science
Open Access Proceedings

A Novel Target-Height Estimation Approach Using Radar-Wave Multipath Propagation for Automotive Applications

Amir Laribi[1], Markus Hahn[1], Jürgen Dickmann[1], and Christian Waldschmidt[2]

[1]Daimler AG, Research Center Ulm, Environment Perception, Ulm, Germany
[2]Ulm University, Institute of Microwave Techniques, Ulm, Germany

Correspondence to: Amir Laribi (amir.laribi@daimler.com)

Received: 22 December 2016 – Accepted: 27 March 2017 – Published: 21 September 2017

Abstract. This paper introduces a novel target height estimation approach using a Frequency Modulation Continuous Wave (FMCW) automotive radar. The presented algorithm takes advantage of radar wave multipath propagation to measure the height of objects in the vehicle surroundings. A multipath propagation model is presented first, then a target height is formulated using geometry, based on the presented propagation model. It is then shown from Sensor-Target geometry that height estimation of targets is highly dependent on the radar range resolution, target range and target height. The high resolution algorithm RELAX is discussed and applied to collected raw data to enhance the radar range resolution capability. This enables a more accurate height estimation especially for low targets. Finally, the results of a measurement campaign using corner reflectors at different heights are discussed to show that target heights can be very accurately resolved by the proposed algorithm and that for low targets an average mean height estimation error of 0.03 m has been achieved by the proposed height finding algorithm.

1 Introduction

On the road to autonomous driving, it has become clear that height information of objects in the car's surroundings is of major importance for collision avoidance systems. Consider for example a situation where, based on received radar data, a collision avoidance system has to decide if a detected target ahead represents an imminent collision threat and therefore breaking has to be initiated or the target is merely a traversable bridge. A similar situation where height information is needed, is during automated parking scenarios. When autonomously executing valet parking for example, the parking pilot has to drive the car through a complex environment and safely reach it's parking lot or garage. On the way to its destination, the parking pilot could encounter different objects as shown in Fig. 1 where a decision has to be made on whether the object is traversable so the car can continue driving without any human, environment or self-damage, or whether the object is an obstacle requiring the driving pilot to choose either to maneuver the car away in order to avoid collision or to stop when no other option is available.

Besides the importance of height information for collision avoidance systems, knowing the target height of reflecting objects in the surrounding environment is very beneficial for self localization. Extending maps from 2-D to 3-D allows more accurate localization and less ambiguity when performing registration, for example in Simultaneous Localization and Mapping applications, and hence provides a better driving environment representation.

Recently, many approaches in different fields have been proposed to estimate target heights in multipath environments. For maritime surveillance applications, simulation results of a study conducted to estimate the height of marine targets were provided in Habonneau et al. (2013b, a). The approach consisted of estimating temporal delays between neighboring paths of a multipath propagation pattern over the sea surface to approximate the height of a target reflector. For air surveillance applications, a multipath height finding method using a narrow band stepped frequency radar was proposed in Phu et al. (2007), where a state space based approach was used to fuse measurements from multiple sets of narrowband radar returns randomly stepped in frequency to estimate height of aircraft. In Berube et al. (2007) the Airborne Warning and Control System (AWACS) radar capabilities were extended to achieve multipath height finding over

Published by Copernicus Publications on behalf of the URSI Landesausschuss in der Bundesrepublik Deutschland e.V.

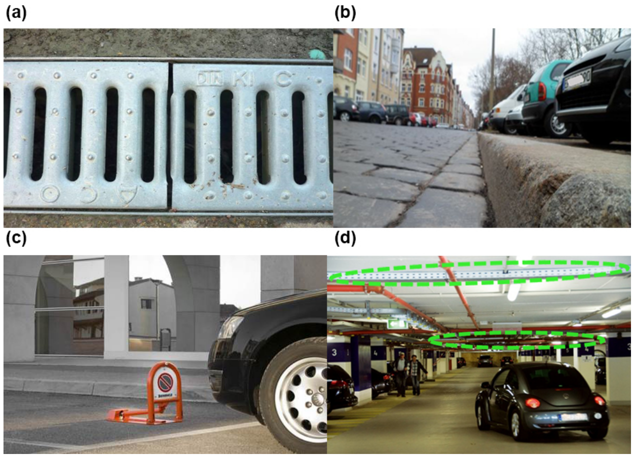

Figure 1. Different automated parking scenarios where height estimation of objects is necessary. **(a)** Rain channel drain is a traversable object which is present in many driving environments, without information about its height it could be interpreted as an obstacle. Sometimes a self driving car has to drive over a curb **(b)** to reach a parking lot, to achieve this, the parking pilot has to know if the curbstone height is low enough (traversable) or not. **(c)** Shows a transit lock. A traversable ceiling element **(d)**, again, without height information the parking pilot would not know whether a detected ceiling element is a traversable object or an obstacle.

land, by processing high range resolution multipath echoes of an airborne target based on available Digital Terrain Elevation Data (DTED). Further, a bridge identification algorithm Diewald et al. (2011) based on a multipath interference pattern was proposed for automotive applications. The used pattern consisted of variation in the backscattered power which is caused by the phase differences of the direct path to the target and the indirect path, during the approaching of bridges or stationary obstacles. Further, signal processing techniques like digital beam forming Barton (1980) and monopulse Si et al. (1999) can be used in combination with Multiple Input Multiple Output radar to measure the elevation angle of a detected target by processing data received from two or more antennas. However while the monopulse approach needs two antenna elements to determine target height, it has no angular resolution. Digital beam forming approaches provide angular estimation at the cost of a higher number of antenna elements. Increasing the number of antennas in turn means more expensive and complex hardware. Moreover both approaches also depend on the radar range resolution when estimating the height of targets that are close to each other, or in the case where the target is an extended object. In this work a height finding algorithm is presented, the algorithm uses radar wave multipath propagation to provide an accurate height estimation of detected targets using a single fixed radar antenna.

The remainder of this work is organized as follows. In Sect. 2, the multipath propagation model of radar waves is

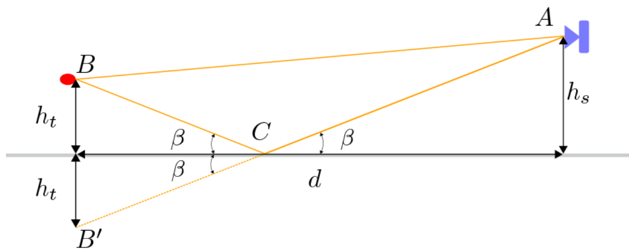

Figure 2. Geometry for radar multipath propagation over a planar reflecting surface.

described and a target height approximation is formulated using geometry. In Sect. 3 the multipath target height estimation using FMCW Radar is discussed and the usefulness of the high resolution algorithm RELAX for the accuracy improvement of the proposed height finding algorithm is shown. In Sect. 4 the radar measurement setup is described, then summarized and the results of the measurements are discussed. Section 5 contains the conclusion.

2 Multipath Propagation Model

In this section the multipath propagation model of radar waves (Fig. 2) is described, then a height approximation of a detected target is formulated based on geometry. Assuming a smooth and perfectly reflecting flat earth, the energy radiated by the radar antenna (A) travels along two separate paths and reaches a point target (B). The first one is the direct path (AB), the second is the indirect path (ACB) that includes a forward scatter reflection from the surface at point (C). The signal reflected by the target also arrives back at the radar by the same two paths. Therefore, there are four components to a multipath echo Skolnik (2001). The first component is (ABA), i.e the round trip along the direct path and the return over the same path (BA). The second one (ABCA) corresponds to the travel along the direct path (AB) and back to the radar along the indirect path (BCA). The third component (ACBA) has the same length as (ABCA) but an opposite path, the radar waves travel along the indirect path (ACB) first then return via the direct path (BA). The fourth component (ACBCA) is the round trip along the indirect path (ACB) and back over the same path (BCA). Therefore, the magnitude of the resultant echo signal back at the radar antenna depends on the magnitudes and the phases of the signals that propagate via the direct and the surface scattered paths.

Using geometry the path length of (AB) can be formulated as follows:

$$\mathrm{AB} = [d^2 + (h_\mathrm{s} - h_\mathrm{t})^2]^{\frac{1}{2}} = d[1 + \frac{(h_\mathrm{s} - h_\mathrm{t})^2}{d^2}]^{\frac{1}{2}}, \quad (1)$$

where d is the ground distance between the radar and the target, and h_s and h_t are the respective heights of the radar sensor and the target. Assuming that $|h_s - h_t| \ll d$, Eq. (1) can be written using Taylor expansion as described in Skolnik (2001).

$$AB \approx d[1 + \frac{1}{2}\frac{(h_s - h_t)^2}{d^2}] = d + \frac{(h_s - h_t)^2}{2d}. \quad (2)$$

Assuming that $|h_t + h_s| \ll d$, the surface reflected path length ACB is given by the following equation

$$ACB' = ACB = [d^2 + (h_s + h_t)^2]^{\frac{1}{2}} \approx d + \frac{(h_t + h_s)^2}{2d}. \quad (3)$$

The difference between the two paths Δr is given by

$$\Delta r = ACB - AB = \frac{2h_t h_s}{d}. \quad (4)$$

Assuming the ground distance d can be replaced by the radial distance R, Eq. (4) can be rewritten as:

$$\Delta r \approx \frac{2h_t h_s}{R}. \quad (5)$$

3 Multipath Height Estimation using FMCW Radar

In this section the multipath target height estimation using FMCW Radar will be discussed. As shown in the previous section, the target height can be formulated as follows:

$$h_t \approx \frac{\Delta r R}{2h_s}. \quad (6)$$

From Eq. (6) it can be concluded that for a fixed sensor height h_s, h_t depends on the target range R and the range difference Δr. When the range is also fixed, the target height is dependent only on Δr. Hence the task of determining the height of a target using multipath propagation consists of accurately determining the range difference Δr in addition to the target range. When using FMCW radar, the target range, that is the distance from sensor to target along the direct path, corresponds to a peak located at a frequency f_{b_1} in the frequency domain, this frequency is also known as the beat frequency, and is related to the range by the following equation:

$$R = \frac{T_d c}{2B} f_{b1}, \quad (7)$$

where T_d denotes the chirp duration, c the speed of light and B the radar bandwidth. In the multipath case, a second peak located at a frequency f_{b_2} close to the main peak is also resolved. This second peak is the result of the round trip along the indirect path (ACB), thus its frequency is always higher than the main beat frequency. The offset Δf_b between these two frequencies corresponds to Δr in the range domain, as seen in Fig. 3. From Eq. (6) it can be deduced that Δr can be very small when detecting a low target or when the detected target is located at long range. This is manifested in the frequency domain as the offset Δf_b also being small. If Δr is smaller than the range resolution of the sensor, the second peak f_{b_2} merges with the main peak f_{b1} in the range domain, so the range separation Δr can-not be resolved anymore, as shown in Fig. 4. This in turn means that the target height can no longer be measured.

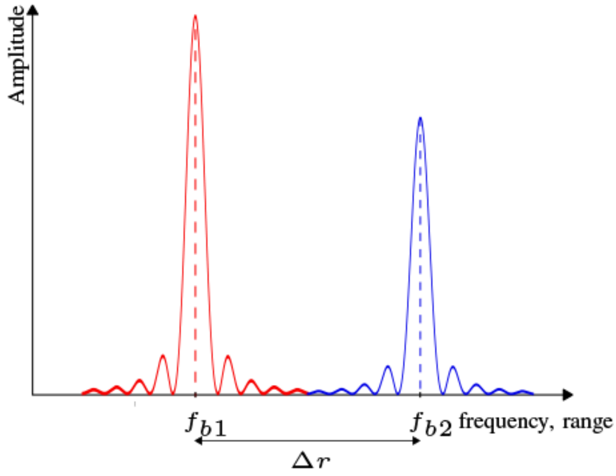

Figure 3. Two beat frequencies corresponding to two echoes from a detected point target in a multipath environment, f_{b_1} (colored red) results from the reflection of the target along the direct Path (AB), f_{b_2} (colored blue) is the reflection of the target along the indirect Path (ACB), Δr is the range separation between the two frequencies.

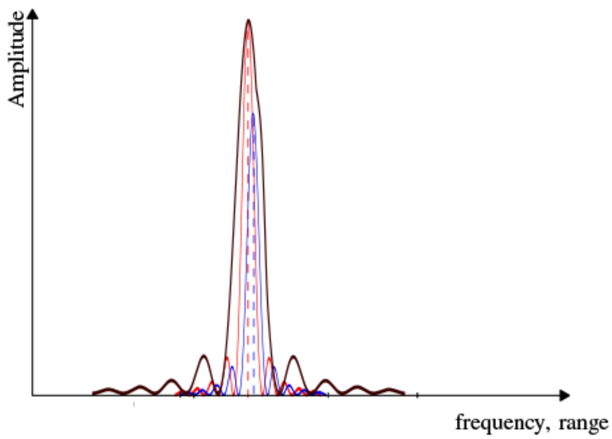

Figure 4. The beat frequency f_{b_2} (colored blue) is very close to the main frequency f_{b_1} (colored red) so that the frequency offset Δ_{f_b} is smaller than the radar range resolution, hence f_{b_2} is merged with f_{b_1}.

High resolution spectral analysis methods Stoica and Moses (1997, 2005) can improve the frequency resolution so that target heights can still be measured even when Δr is smaller than the actual sensor range resolution. In this work

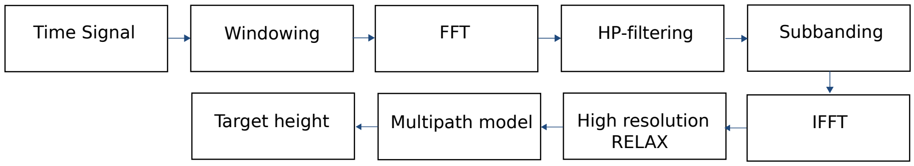

Figure 5. Block Diagram showing the processing steps of the multipath height finder algorithm.

Figure 6. Measurement setup.

the RELAX algorithm was implemented and used to enhance the multipath peaks spectral resolution.

3.1 Usage of RELAX for Multipath Height-Finding

RELAX Li and Stoica (1996) is a parametric high resolution algorithm which relies on a nonlinear regression model to estimate the frequencies present in a signal as well as their respective amplitudes. RELAX is an asymptotically statistically efficient estimator which converges even when the signal is affected by unknown colored noise. In this section the problem of 1-D parameter estimation of K complex sinusoids is addressed. The RELAX algorithm assumes that received radar signal y can be modeled as the sum of multiple weighted complex exponentials plus noise, this means that the received signal can be described by the following model:

$$y_n = \sum_{k=1}^{K} \alpha_k e^{j2\pi f_k n} + e_\mathrm{n}. \tag{8}$$

here, $n = 0, 1, \ldots, N-1$ with N denoting the number of the data samples, α_k and f_k denote the unknown complex amplitude and unknown frequency of k-th harmonic respectively for $k = 1, 2, \ldots, K$; e_n denotes the noise. The sinusoidal parameters $\{\hat{f}_k, \hat{\alpha}_k\}$ can be obtained by recursively minimizing the following nonlinear least-squares cost function

$$C_l(\{f_i, \alpha_i\})_{i=0}^{K} = \| y - \sum_{k=1}^{K} \alpha_k w(f_i) \|^2, \tag{9}$$

where $\|.\|$ denotes the Euclidean norm,
$y = [y_0\ , y_1\ \ldots\ , y_{N-1}]^T$, and

$$w(f_k) = [1\ \ e^{j2\pi f_k}\ \ldots\ e^{j2\pi f_k (N-1)}]^T. \tag{10}$$

Consider the following simple preparations, let

$$y_k = y - \sum_{i=1, i\neq k}^{K} \hat{\alpha}_i w(\hat{f}_i), \tag{11}$$

where $\{\hat{f}_i, \hat{\alpha}_i\}_{i=1, i\neq k}^{K}$ are assumed to be given then, minimizing the cost function in Eq. (9) with respect to f_k and α_k gives Li (1998)

$$\begin{aligned} \hat{f}_k &= \min_{f_k} \| [I - \frac{w(f_k) w^H(f_k)}{N}] y_k \|^2 \\ &= \max_{f_k} | w^H(f_k) y_k |^2 \end{aligned} \tag{12}$$

and

$$\hat{\alpha}_k = \left. \frac{w^H(f_k) y_k}{N} \right|_{f_k = \hat{f}_k}. \tag{13}$$

This means that $\hat{f}_k$ can be obtained as the location of the dominant peak of the periodogram $|w^H(f_k) y_k|^2/N$, which can be efficiently computed by using the FFT with the data sequence y_k padded with zeros. Then, α_k is computed from the complex height of the peak of $w^H(f_k) y_k/N$. Hence the relaxation algorithm for the minimization of the nonlinear least-squares cost function can be summarized into the following steps Li (1998):

- Step 1: Assume $K = 1$, obtain $\hat{f}_1$ and $\hat{\alpha}_1$ from y using Eqs. (12) and (13) with y_k from replaced by y
- Step 2: Assume $K = 2$, compute y_2 with Eq. (11) by using $\hat{f}_1$ and $\hat{\alpha}_1$ obtained in Step 1, obtain $\hat{f}_2$ and $\hat{\alpha}_2$ from y_2 using Eqs. (12) and (13), next compute y_1 (Eq. 11) by using $\hat{f}_2$ and $\hat{\alpha}_2$ and redetermine $\hat{f}_1$ and $\hat{\alpha}_1$ from y_1 by using Eqs. (12) and (13). Iterate the previous two sub steps until "practical convergence" is achieved (to be discussed later on).
- Step 3: Assume $K = 3$, compute y_3 with Eq. (11) by using $\{\hat{f}_i, \hat{\alpha}_i\}_{i=1}^{2}$ obtained in Step 2. Obtain $\hat{f}_3$ and $\hat{\alpha}_3$ from y_3 by using Eqs. (12) and (13). Next, compute y_1 with Eq. (11) by using $\{\hat{f}_i, \hat{\alpha}_i\}_{i=2}^{3}$, and redetermine $\hat{f}_1$

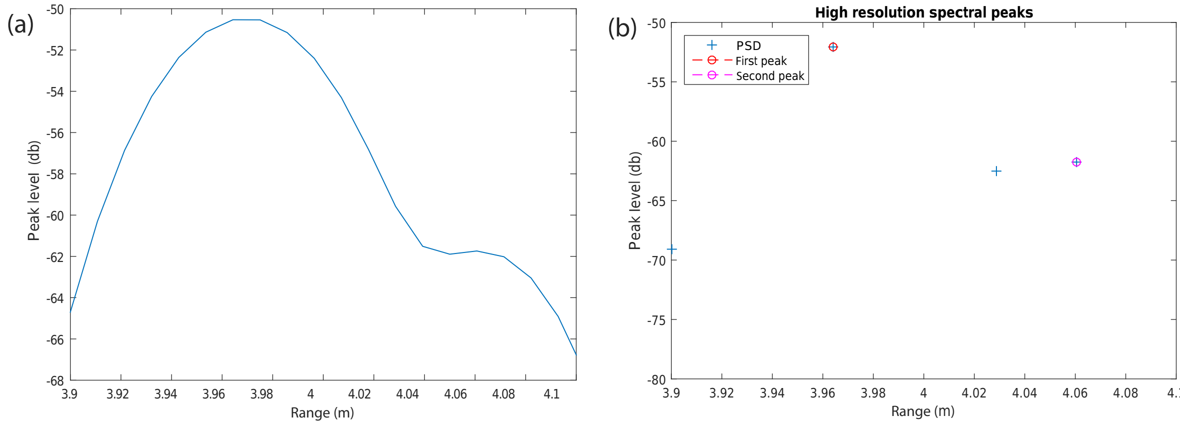

Figure 7. (a) A target (corner reflector) subband computed using FFT. The peaks correspond to a multipath return of a 0.29 m high target located at 4 m range, the indirect multipath peaks are merged with the main peak, hence, they could not be detected using local maxima. **(b)** Output of the height finder showing the RELAX processed version of the subband in **(a)** with two detected peaks (direct peak and indirect peak), the merged frequencies in **(a)** are outputted as line spectra after performing RELAX, hence the detection of the multipath peaks becomes possible.

Table 1. Mean error table of the estimated target heights. the mean error was calculated for 10 height measurements per range for each corner reflector height (256 × 10 chirps), the last row of the table is the average of mean errors for a target height over all ranges (256 × 10 × 7 chirps).

		Target height (Ground truth)/m				
		0.29	0.6	0.9	1.2	1.44
Range (m)	5	0.0526	0.0169	0.0075	0.0043	0.0100
	4.5	0.0937	0.0031	0.0470	0.0266	0.0025
	4	0.0394	0.0051	0.0075	0.0482	0.0739
	3.5	0.0420	0.0329	0.0049	0.0760	0.0907
	3	0.0051	0.0017	0.0103	0.0821	0.6800
	2.5	0.0035	0.0102	0.0750	0.0977	0.7704
	2	0.0041	0.0218	0.5126	0.4372	0.8013
Average mean error		0.0343	0.0131	0.0950	0.1103	0.3470

and $\hat{\alpha}_1$ from y_1. Then, compute y_2 with Eq. (11) by using $\{\hat{f}_i, \hat{\alpha}_i\}_{i=1,3}$ and redetermine $\hat{f}_2$ and $\hat{\alpha}_2$ from y_2. Iterate the previous three sub steps until "pratical convergence".

Remaining Steps. Continue similarly until K is equal to the desired or estimated number of sinusoids.

3.2 The Multipath Height-Finder Algorithm

Figure 5 shows a block diagram which summarizes the processing steps of the proposed multipath height finder algorithm. The algorithm processes $N = 256$ frames to yield a single height estimation. First, the N frames are summed to improve the Signal to Noise Ratio, the resulting time signal is multiplied with a Hanning window and the Power Spectrum Density (PSD) is computed using the Fast Fourier Transform. The PSD is then taken to the range domain, where high energy caused by self-mixing and 1/f noise at ranges up to 0.4 m is removed using a high pass filter. The target subband is selected by adaptively thresholding the PSD magnitude then applying a bandpass filter. Next, the subbanded spectrum is transformed back to the time domain using the Inverse Fourier Transform and a high resolution PSD estimation is obtained using RELAX. After that, the main peak (direct path return) and the second peak (longest indirect path return) are detected in the estimated high resolution PSD where the first peak is chosen as the beat frequency peak with the highest magnitude. Because the indirect path is always longer than the direct path, the second peak is chosen as the second highest peak magnitude with a range greater than the range of the main peak. Finally the target height is estimated using the multipath propagation model in Eq. (6). The output of the height finder algorithm is shown in Fig. 7b.

4 Experimental Results

In this section the radar measurement setup is described and the results of the measurement are summarized and discussed.

4.1 Measurement Setup

In the following experiment a 77 GHz short range FMCW radar with 3 GHz bandwidth was used, the radar sensor was placed 0.56 m above the ground. A 10 dBsm corner reflector was used as target, the height of the corner reflector was varied from a lowest possible height of 0.29 m to a maximum height of 1.44 m with a height step of approximately 0.3 m. At each height step the range of the corner reflector was varied from 2 to 5 m in 0.5 m step. At each range step 2560 received frames were recorded. The algorithm processed 256 received frames to yield a single height estimation.

4.2 Results

Table 1 shows the mean error of 10 heights estimations per single range and target height step, i.e the difference $h_g - h_m$ between ground truth and the average of 10 measured heights (or the average of 256 × 10 chirps), where h_g and h_m denote the ground truth height and the average measurement respectively. Note that no absolute value was applied to the difference, i.e the measured heights were always below or nearly equal to the corresponding ground truth heights, the mean errors for a single target height are averaged again in the last row of the Table to yield an average of mean errors over all ranges for one target height, i.e the average of 256 × 10 × 7 chirps. As shown in the Table, the height-finding algorithm can resolve target heights with very high accuracy when both the Taylor approximation constraint and the distance approximation assumption are fulfilled. For small targets $h_t \leq 0.9$ m these constraints still apply even at close range. Hence it can be seen from the table that the mean error for low targets located at short range is very small, the error becomes a bit higher for measurements at longer range, because the multipath range difference Δr gets smaller with increasing range between sensor and target. However, the mean error was still smaller than 0.1 m. The performance of the algorithm degrades for higher target heights $h_t \geq 0.9$ m which are located at short ranges $R \leq 3$ m, this is due to the fact that for short distances and high targets the assumption for the Taylor approximation needed for Eqs. (2) and (3) no longer holds, moreover the assumption that the ground distance d can be approximated by the radial distance R is also not valid anymore. However despite these errors the algorithm still delivers enough information so that at any time, the parking pilot could know if the target ahead is traversable or not. It can be seen from Table 1 that at sufficient range $R \geq 3.5$ m the height measurements of these targets become more accurate and nearly reach ground truth at ranges $R \geq 4.5$ m.

5 Conclusions

In this work a multipath height finder algorithm using a 77 GHz short range FMCW radar was proposed. Measurement results carried with a 10 dBsm corner reflector were shown and discussed. For small targets ($h_t = 0.29$ m) an average mean height estimation error of 0.03 m has been achieved by the height-finder algorithm. It can be concluded that height estimation of short range point targets can be resolved with high accuracy by harnessing the multipath propagation of radar waves. The goal of determining whether a detected point target is traversable or not was successfully achieved by the proposed algorithm. Subsequent work will focus on height finding of extended targets using radar wave multipath propagation.

Data availability. A Public access to the data is not possible due to a non-disclosure agreement (NDA) with the company, concerning the used hardware and data.

Competing interests. The authors declare that they have no conflict of interest.

Acknowledgements. The research leading to these results has received funding from the European Commission Seventh Framework Programme (FP/2007-2013) under the project AdaptIVe, grant agreement number 610428. Responsibility for the information and views set out in this study lies entirely with the authors. The authors would like to thank all partners within AdaptIVe for their cooperation and valuable contribution.

Edited by: J. Anders
Reviewed by: two anonymous referees

References

Barton, P.: Digital beam forming for radar, Communications, Radar and Signal Processing, IEE Proc.-F, 127, 266–277, 1980.

Berube, C. D., Felcyn, P. R., Hsu, K., Latimer, J. H., and Swanay, D. B.: Target height estimation using multipath over land, in: 2007 IEEE Radar Conference, 88–92, IEEE, 2007.

Diewald, F., Klappstein, J., Sarholz, F., Dickmann, J., and Dietmayer, K.: Radar-interference-based bridge identification for collision avoidance systems, in: Intelligent Vehicles Symposium (IV), 2011 IEEE, 113–118, IEEE, 2011.

Habonneau, J., Le Caillec, J.-M., Khenchaf, A., and Mandridake, L.: Multipath height estimation of target reflectors, in: 2013 14th International Radar Symposium (IRS), 1, 258–263, IEEE, 2013a.

Habonneau, J., Le Caillec, J.-M., Khenchaf, A., and Mandridake, L.: A study of performances of multipath height estimation algorithm for marine target imaging, in: Radar (Radar), 2013 International Conference on, 48–53, IEEE, 2013b.

Li, J.: Implementation of the RELAX algorithm, IEEE T. Aero. Elec. Sys., 34, 657–664, 1998.

Li, J. and Stoica, P.: Efficient mixed-spectrum estimation with applications to target feature extraction, IEEE T. Signal Proces., 44, 281–295, 1996.

Phu, P., Aumann, H., and Piou, J. E.: Multipath height finding in the presence of interference, in: 2007 IEEE Antennas and Propagation Society International Symposium, 2007.

Si, D., Luo, S. C., Pero, C., Wu, X., and Knox, R.: Millimeter-wave FMCW/monopulse radar front-end for automotive applications, in: Microwave Symposium Digest, 1999 IEEE MTT-S International, 1, 277–280, IEEE, 1999.

Skolnik, M.: Introduction to Radar systems, IEEE Aero. El. Sys. Mag., 16, 19–19, 2001.

Stoica, P. and Moses, R. L.: Introduction to spectral analysis, vol. 1, Prentice hall Upper Saddle River, 1997.

Stoica, P. and Moses, R. L.: Spectral analysis of signals, Pearson/Prentice Hall Upper Saddle River, NJ, 2005.